# SUPPLEMENTAL INFORMATION

## Assembly of excitatory synapses in the absence of glutamatergic neurotransmission.

Richard Sando, Eric Bushong, Yongchuan Zhu, Min Huang, Camille Considine, Sebastien Phan, Suyeon Ju, Marco Uytiepo, Mark Ellisman and Anton Maximov

Inventory of Supplemental Information

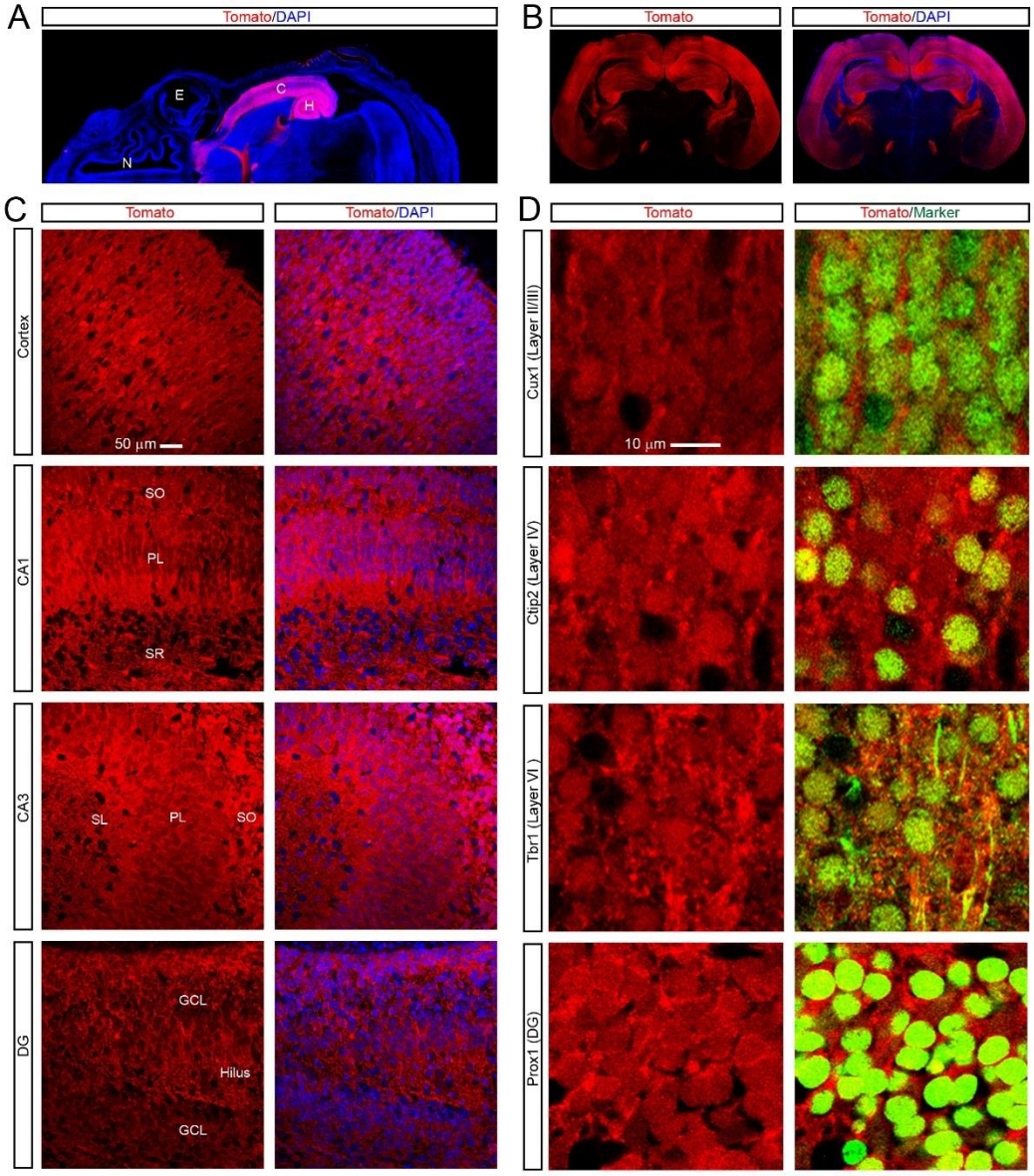


**Figure S1 (Related to Figure 1) Recombinase activity of *Emx1*$^{IRES\text{-}Cre}$.**

Recombinase activity of *Emx1*$^{IRES\text{-}Cre}$ was assessed with the *Ai9* tdTomato Cre reporter in brains of neonatal (p1) *Emx1*$^{IRES\text{-}Cre}$/*Ai9* mice. **(A** and **B)** Confocal images of tdTomato fluorescence in DAPI-stained sections across the head (panel A) and the brain (panel B). **(C)** Higher-magnification images of coronal brain sections show wide-spread induction of reporter expression in the cerebral cortex and hippocampus. SO = stratum oriens; SR = stratum radiatum, SL = stratum lucidum; PL = pyramidal cell layer; GCL = granule cell layer. **(D)** Sections were imaged after labeling with antibodies against different subtypes of glutamatergic neurons (shown in green). Cux1: cortical layers II/II; Ctip2: cortical layer IV; Tbr1: cortical layer V; Prox1: dentate granule cells (GCs).

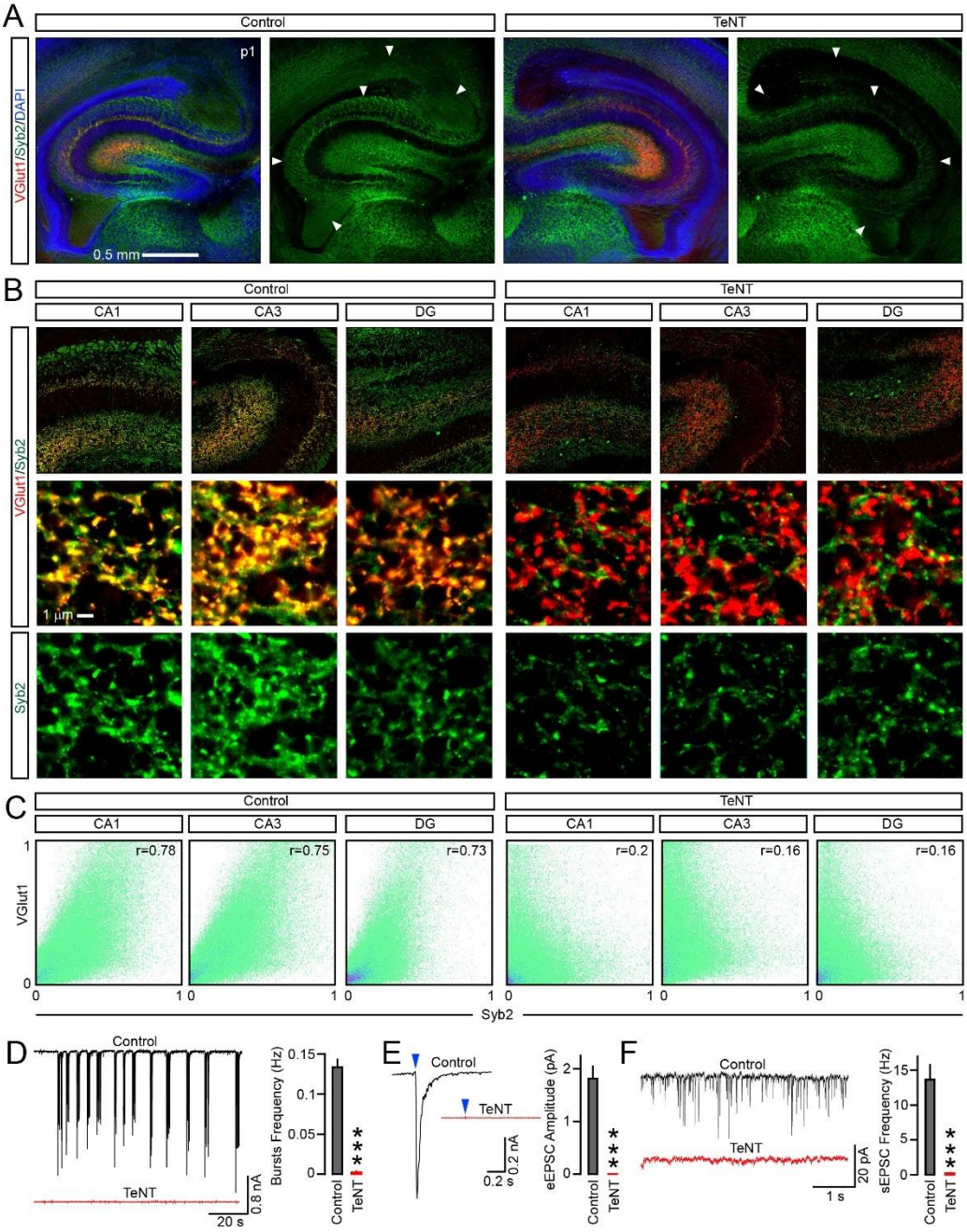


**Figure S2 (Related to Figure 1). Distribution of Syb2 in the forebrain of neonatal Emx1/TeNT mice.**

**(A** to **C)** Coronal brain sections from p1 control and Emx1/TeNT mice were co-labeled with DAPI and antibodies against Syb2 (green) and a marker of glutamatergic presynaptic terminals, VGlut1 (red). **(A** and **B)** Images at different magnification demonstrate the TeNT-dependent loss of Syb2 in excitatory fiber tracts (arrows in panel A) and nascent VGlut1-positive presynaptic boutons across the hippocampus (panel B). High magnification frames were acquired from stratum radiatum of the CA1, stratum lucidum of the CA3 and molecular layer of the dentate gyrus (DG). **(C)** Colocalization of VGlut1 and Syb2 in the CA1, CA3 and DG. Pseudo colored pixel intensity graphs and Person's correlation coefficients (r) demonstrate the extent of overlap of two fluorophores in $100^2$ µm image frames. **(D** to **F)** Vesicular release of glutamate in cultured neurons. Dissociated cultures were prepared from cortices of p1 pups and maintained *in vitro* for 15 days (DIV15). Whole-cell voltage-clamp recordings were performed in the presence of the GABA receptor blocker, picrotoxin (100 µM). Holding potentials were -70 mV. Panels show sample traces and averaged values from 3 mice/cultures per genotype, plotted as mean ± S.E.M. ***$P < 0.00001$ (Student's *t*-test). **(D)** Network activity was monitored in the absence of stimulation. **(E)** Evoked AMPA-type excitatory postsynaptic currents (eEPSCs) were triggered by isolated action potentials. Arrows mark times of stimulation with the local extracellular electrode. eEPSC amplitude: Control, $n = 17$ neurons; TeNT, $n = 21$. **(F)** Spontaneous fusion of single neurotransmitter vesicles. sEPSC frequency: Control, $n = 17$; TeNT, $n = 20$. See also Table S1 for additional analyses and statistics.

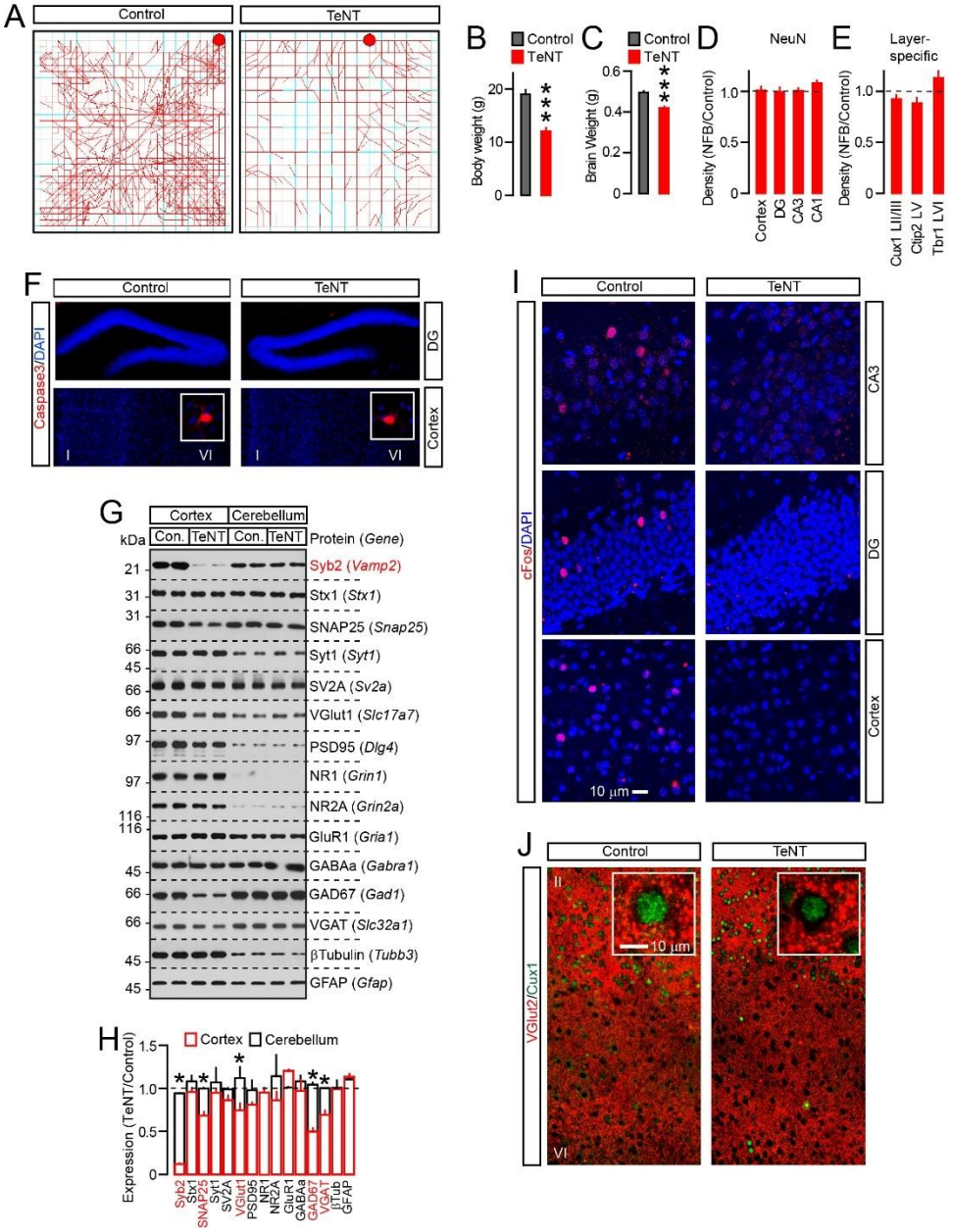


**Figure S3 (Related to Figure 1). Characterization of Emx1/TeNT mice.**

Emx1/TeNT mice and their normal littermate controls were examined at 4 weeks of age.

**(A)** Examples of locomotor activity in the open field, assessed for 30 min with infrared sensors in a sound-proof 45x45 cm box. See also Movies S1 and S2. **(B** and **C)** Body and brain weights. Representative images are shown in main Figure 1G. Body weights: Control, $n = 11$ mice; TeNT, $n = 10$. Brain weights: Control, $n = 9$; TeNT, $n = 9$. Graphs are plotted as mean ± S.E.M. ***$P < 0.0001$ (Student's $t$-test). **(D)** Densities of NeuN-positive cells across the column of the somatosensory cortex and in granule and pyramidal cell layers of the the DG, CA3 and CA1. Cortex: $P = 0.9$; DG: $P = 0.86$; CA3: $P = 0.93$; CA1: $P = 0.12$. Representative images are shown in Figure 1H. **(E)** Densities of Cux1-, Ctip2- and Tbr1-positive cells in cortical layers II/III, IV and VI, respectively. Cux1: $P = 0.14$; Ctip2: $P = 0.23$; Tbr1: $P = 0.03$. Representative images are shown in Figure 1I. In panels D and E, data from 3 pairs of mice (3-7 sections per animal) are plotted as TeNT/Control ratio, mean ± S.E.M. **(F)** Coronal brain sections were labeled with DAPI and an antibody against cleaved Caspase3. Images of the DG and somatosensory cortex are shown. **(G** and **H)** Expression of synaptic proteins, βTubulin and GFAP in the cortex and cerebellum (as an internal control) of normal and Emx1/TeNT mice. Protein homogenates were isolated at p30 and probed by immunoblotting with indicated antibodies. **(G)** Representative immunoblots from 2 pairs of mice. **(H)** Quantifications of protein levels, represented as TeNT/Control ratio, mean ± S.E.M. ($n = 3$ mice/genotype). *$P < 0.05$ (Student's $t$-test). Reduction of VGlut1 and VGAT likely reflects reduced synapse numbers (see Figure 2). Expression of SNAP25 and GAD67 is known to be influenced by neuronal activity. **(I)** Images of indicated brain regions in sections that we labeled with DAPI and antibody against cFos (red). **(J)** Images of cortical columns in sections that were labeled with antibodies against VGlut2 (red) and Cux1 (green). Inserts show VGlut2-positive terminals in superficial layer II at higher magnification.

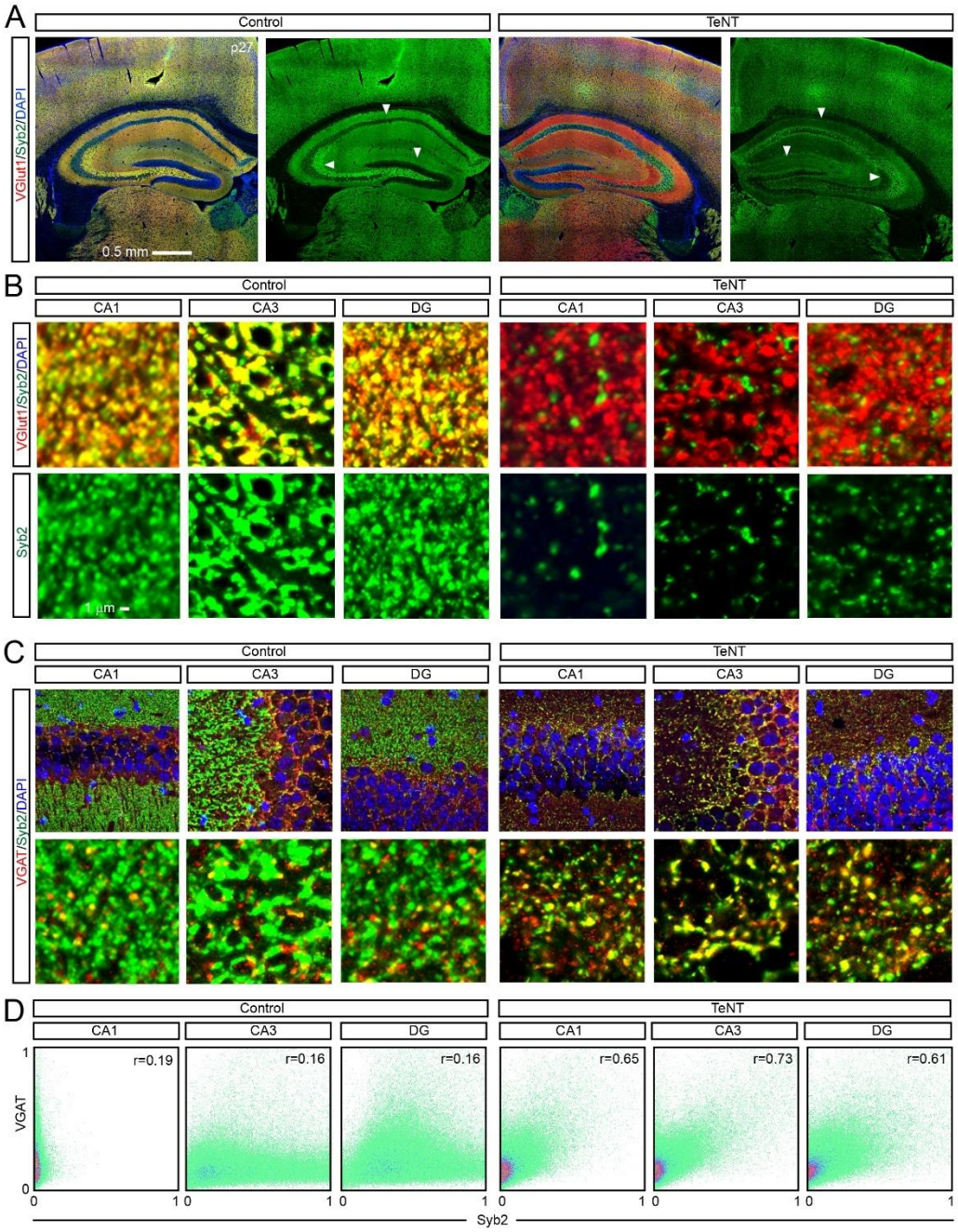


**Figure S4 (Related to Figure 2). Distribution of Syb2 in the hippocampus of 4 weeks old Emx1/TeNT mice.**

Analysis of Syb2 immunoreactivity in presynaptic terminals of glutamatergic and inhibitory GABAergic neurons in the hippocampi of 4 weeks old control and Emx1/TeNT mice. Brain sections were imaged after labeling with DAPI and indicated antibodies.

**(A** and **B)** Images at different magnification demonstrate the TeNT-dependent loss of Syb (green) in VGlut1-positive excitatory synapses (red) across the hippocampus. High magnification frames were acquired from stratum radiatum of the CA1, stratum lucidum of the CA3 and molecular layer of the DG. Additional imaged and quantifications are shown in Figure 2. **(C** and **D)** Samples were labeled for Syb2 (green) and inhibitory synapse marker, VGAT (red). **(C)** Images at different magnification demonstrate that, in Emx1/TeNT mice, the remaining Syb2 puncta overlaps with VGAT, reflecting efficient cleavage in excitatory neurons and lack of TeNT expression in interneurons. **(D)** Quantitative analysis of colocalization of VGAT and Syb2 in the CA1, CA3 and DG. Pseudo colored pixel intensity graphs and Person's correlation coefficients (r) demonstrate the extent of overlap of two fluorophores in $100^2$ µm image frames taken from perisomatic regions.

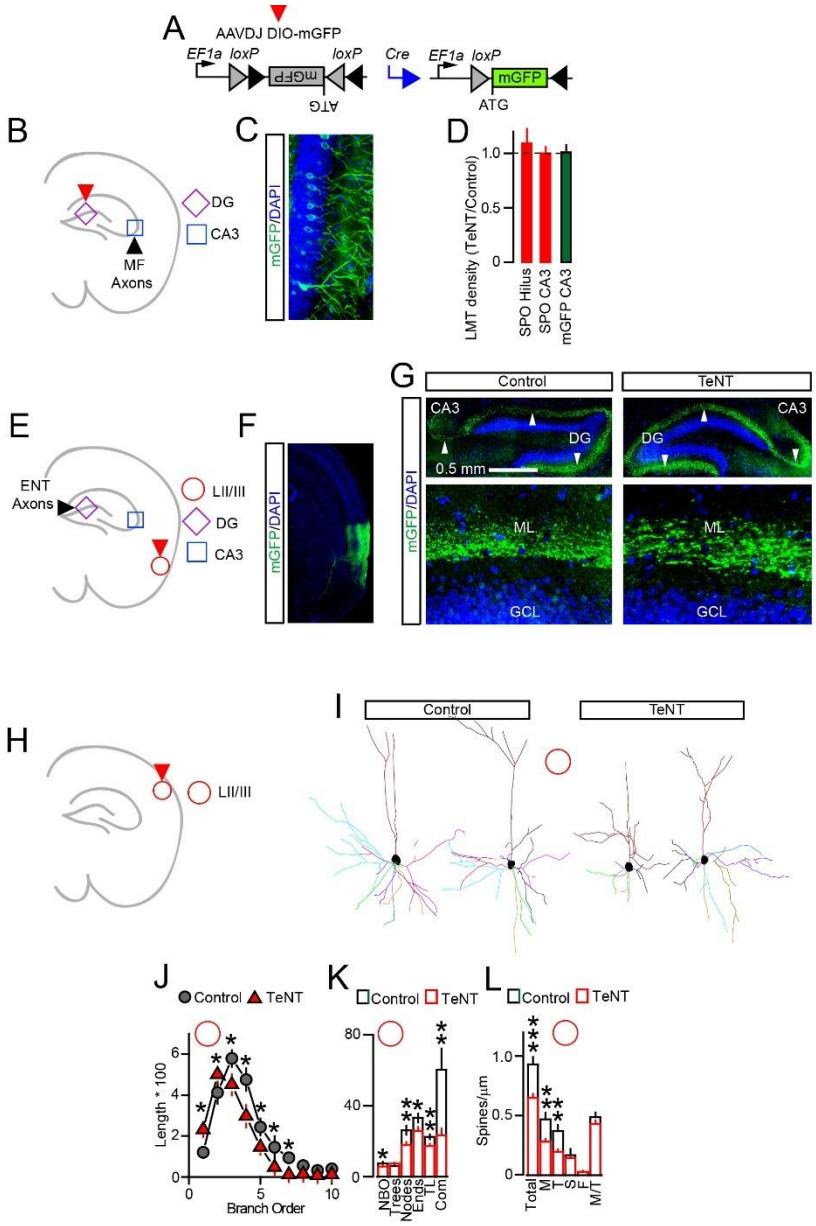


**Figure S5 (Related to Figures 2 and 3). Viral tracing of axons and dendrites of single neurons.**

Long-range projections and morphologies of single excitatory neurons were visualized using Cre inducible expression of membrane-bound GFP from an AAV (AAVDJ DIO-mGFP). Animals were injected with viruses at p3 to achieve labeling of dentate GCs or pyramidal cells in superficial layers of the entorhinal and somatosensory cortex, as shown in panels B, E and H. Confocal imaging of brain sections was performed at p30.

**(A)** Schematics of mGFP induction in neurons carrying Cre. **(B** and **C)** Sites of reporter expression/imaging and specificity of GC targeting in the DG for analysis of mossy fiber axons. See also Figure 2D for representative images of mossy fibers in the CA3. **(D)** Total densities of SPO-positive large mossy fiber terminals (LMTs) in the hilus and CA3 and linear densities of mGFP-tagged LMTs per axon length, plotted as TeNT/Control ratio. **(E** to **G)** Imaging of entorhinal axons in the hippocampus. **(E** and **F)** Sites of mGFP expression/imaging (panel E) and specificity of AAV targeting in the cortex (panel F). **(G)** Labeled axons of projection entorhinal layer II/III neurons are shown at different magnifications. Top: axon bundles that project through molecular layer (ML) of the DG and terminate in the CA3 (arrows). Bottom: high magnification images of axonal puncta in the ML. Representative images from two independent experiments are shown. Note no reporter expression in dentate GCs whose somas in the GCL are labeled with DAPI.

**(H** to **L)** Morphologies of pyramidal cells in layer II/III of the somatosensory cortex. **(H)** Sites of mGFP expression/imaging. **(I)** Dendritic trees of single neurons were reconstructed in Neurolucida from 3D image stacks. **(J)** Averaged length of branches of different order (µm * 100). **(K)** Mean numbers of branch orders (NBO), trees, nodes, ends, tree length (TL, µm * 100), and complexity indexes (Com, a.u. *1000). Control, $n$ = 3 mice/15 neurons; TeNT, $n$ = 3/20. **(L)** Linear densities of different spine types on proximal dendrites. M = mushroom; T = thin; S = stubby; F = filopodia; M/T = ratio of mushroom to total. Control, $n$ = 3 mice/20 neurons; TeNT, $n$ = 3/16. All graphs are plotted as mean ± S.E.M. *$P$ < 0.05; **$P$ < 0.01; ***$P$ < 0.001 (Student's $t$-test).

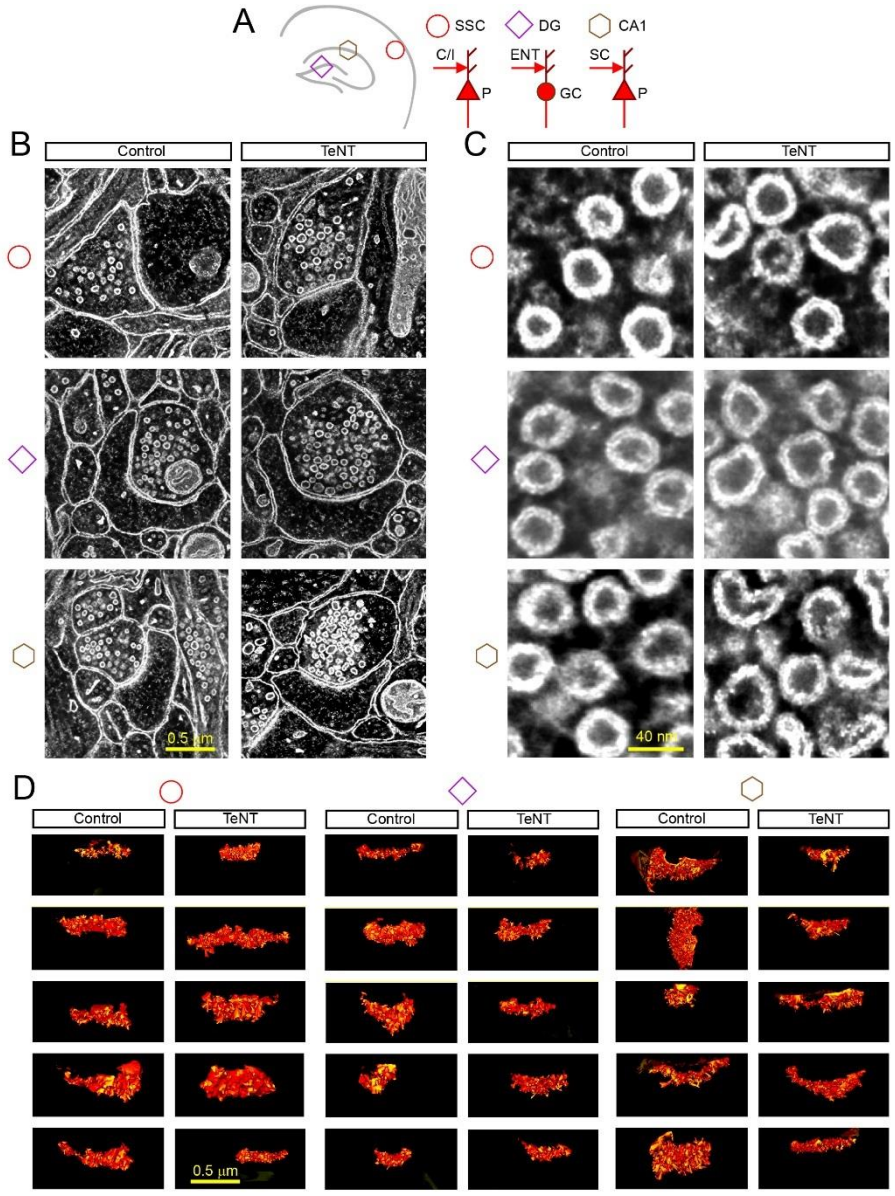


**Figure S6 (Related to Figure 4). SEM analysis of single synapses.**
Structures of single excitatory synapses in stratum radiatum of the CA1, molecular layer of the DG, and layer II/III of the somatosensory cortex of p30 control and TeNT mice were analyzed by SEM tomography.
**(A)** Simplified diagrams of excitatory circuits in examined areas. P = pyramidal neuron; GC = granule cell; C/I = callosal or ascending layer IV afferents; ENT = entorhinal axons; SC = Schaffer collaterals. **(B** and **C)** Typical 2D EM images of synapses (panel B) and neurotransmitter vesicles (panel C) in three brain regions. Note a distortion of vesicle shapes in synapses of animals carrying TeNT. Full 3D reconstructions and quantifications are shown in Figure 4. **(D)** Exampled of postsynaptic densities (PSDs) that were reconstructed from 2D image stacks.

**Table S1. Summary of electrophysiology (Related to Figures 1 and 2).**

| Genotype / Parameter | Mean ± S.E.M. | *P* value | Mice/Cells |
|---|---|---|---|
| **Recordings from cortical neurons in primary cultures (p1+DIV15)** | | | |
| AMPA-type sEPSC frequency (Hz) | | | |
| Control | 13.7 ± 2.1 | | 3/17 |
| Emx1/TeNT | 0.2 ± 0.1 | <0.00001 | 3/20 |
| AMPA-type sEPSC amplitude (pA) | | | |
| Control | 16.4 ± 2.3 | | 3/17 |
| Emx1/TeNT | 20 ± 3.4 | 0.32 | 3/11 |
| AMPA-type eEPSC amplitude (pA) * | | | |
| Control | 1812 ± 234 | | 3/17 |
| Emx1/TeNT | 4 ± 2 | <0.00001 | 3/21 |
| NMDA-type eEPSC amplitude (pA) * | | | |
| Control | 361 ± 47 | | 3/15 |
| Emx1/TeNT | 4 ± 2 | <0.00001 | 3/18 |
| sIPSC frequency (Hz) | | | |
| Control | 3.9 ± 0.6 | | 3/13 |
| Emx1/TeNT | 2.7 ± 0.5 | 0.05 | 3/10 |
| sIPSC amplitude (pA) | | | |
| Control | 18.9 ± 2.5 | | 3/12 |
| Emx1/TeNT | 19.5 ± 4.5 | 0.89 | 3/10 |
| eIPSC amplitude (pA) * | | | |
| Control | 3670 ± 426 | | 3/12 |
| Emx1/TeNT | 2914 ± 470 | 0.14 | 3/10 |
| | | | |
| **Recordings from acute brain slices (p30)** | | | |
| AMPA-type sEPSC frequency (Hz), Cortical layer IV | | | |
| Control | 1.88 ± 0.07 | | 3/6 |
| Emx1/TeNT | 0.5 ± 0.16 | 0.001 | 3/5 |
| AMPA-type sEPSC frequency (Hz), DG | | | |
| Control | 1.13 ± 0.25 | | 3/6 |
| Emx1/TeNT | 0.03 ± 0.03 | <0.00001 | 3/7 |
| AMPA-type sEPSC frequency (Hz), CA3 | | | |
| Control | 1.61 ± 0.22 | | 3/6 |
| Emx1/TeNT | 0 | 0 | 3/5 |
| AMPA-type sEPSC frequency (Hz), CA1 | | | |
| Control | 1.03 ± 0.09 | | 3/4 |
| Emx1/TeNT | 0.03 ± 0.07 | <0.00001 | 3/5 |
| AMPA-type eEPSC amplitude (pA), Cortical layer IV * | | | |
| Control | 758 ± 44 | | 3/8 |
| Emx1/TeNT | 262 ± 21 | <0.00001 | 3/7 |
| AMPA-type eEPSC amplitude (pA), DG * | | | |
| Control | 570 ± 28 | | 3/6 |
| Emx1/TeNT | 3 ± 3 | <0.00001 | 3/7 |
| AMPA-type eEPSC amplitude (pA), CA3 * | | | |
| Control | 697 ± 92 | | 3/6 |
| Emx1/TeNT | 0 | 0 | 3/5 |
| AMPA-type eEPSC amplitude (pA), CA1 * | | | |
| Control | 739 ± 38 | | 3/4 |
| Emx1/TeNT | 0 | 0 | 3/6 |
| NMDA-type eEPSC amplitude (pA), Cortical layer IV * | | | |
| Control | 326 ± 56 | | 3/6 |
| Emx1/TeNT | 103 ± 10 | <0.00001 | 3/7 |
| NMDA-type eEPSC amplitude (pA), DG * | | | |
| Control | 255 ± 23 | | 3/6 |
| Emx1/TeNT | 3 ± 3 | <0.00001 | 3/7 |
| NMDA-type eEPSC amplitude (pA), CA3 * | | | |
| Control | 192 ± 41 | | 3/6 |
| Emx1/TeNT | 0 | 0 | 3/5 |

| | | | |
|---|---|---|---|
| NMDA-type eEPSC amplitude (pA), CA1 * | | | |
| Control | 461 ± 110 | | 3/4 |
| Emx1/TeNT | 0.5 ± 0.5 | <0.00001 | 3/6 |
| AMPA-type eEPSC charge (nA/ms), Cortical layer IV ** | | | |
| Control | 2.4 ± 0.3 | | 3/4 |
| Emx1/TeNT | 0.2 ± 0.03 | <0.00001 | 3/5 |
| AMPA-type eEPSC charge (nA/ms), DG ** | | | |
| Control | 1.4 ± 0.3 | | 3/5 |
| Emx1/TeNT | 0.03 ± 0 | <0.00001 | 3/4 |
| AMPA-type eEPSC charge (nA/ms), CA3 ** | | | |
| Control | 2.7 ± 0.8 | | 3/5 |
| Emx1/TeNT | 0.02 ± 0 | <0.00001 | 3/4 |
| AMPA-type eEPSC charge (nA/ms), CA1 ** | | | |
| Control | 2.2 ± 0.6 | | 3/5 |
| TeNT | 0.02 ± 0.01 | <0.0001 | 3/3 |
| | | | |
| **Recordings from acute brain slices (p3)** | | | |
| AMPA-type eEPSC amplitude (pA), CA1 * | | | |
| Control | 81 ± 65 | | 2/6 |
| Emx1/TeNT | 1 ± 0 | <0.05 | 2/6 |
| NMDA-type eEPSC amplitude (pA), CA1 * | | | |
| Control | 36 ± 25 | | 2/6 |
| Emx1/TeNT | 1 ± 1 | <0.05 | 2/6 |

* Triggered by single action potentials at 0.1 Hz; ** Triggered by 10 action potentials at 10 Hz

**Table S2. Summary of SEM tomography (Related to Figure 4).**

| **Genotype/Parameter** | | | | | |
|---|---|---|---|---|---|
| **Spine volume (nm^3)** | Mean | S.E.M. | Mice | Synapses | *P* value |
| Control Cortex | 6.77E+07 | 8.77E+06 | 3 | 12 | |
| Emx1/TeNT Cortex | 9.46E+07 | 1.08E+07 | 3 | 11 | <0.05 |
| Control DG | 6.61E+07 | 5.98E+06 | 3 | 11 | |
| Emx1/TeNT DG | 1.10E+08 | 1.97E+07 | 3 | 9 | <0.05 |
| Control CA1 | 8.08E+07 | 1.37E+07 | 3 | 10 | |
| Emx1/TeNT CA1 | 1.25E+08 | 1.56E+07 | 3 | 10 | <0.05 |
| **PSD volume (nm^3)** | | | | | |
| Control Cortex | 6.78E+06 | 751097 | 3 | 12 | |
| Emx1/TeNT Cortex | 9.94E+06 | 986638 | 3 | 11 | 0.5269 |
| Control DG | 4.11E+06 | 480015.8 | 3 | 11 | |
| Emx1/TeNT DG | 7.39E+06 | 1.03E+06 | 3 | 9 | <0.01 |
| Control CA1 | 8.17E+06 | 1.39E+06 | 3 | 10 | |
| Emx1/TeNT CA1 | 9.33E+06 | 1.13E+06 | 3 | 10 | <0.02 |
| **PSD/Spine Volume ratio** | | | | | |
| Control Cortex | 0.1179 | 0.02374 | 3 | 12 | |
| Emx1/TeNT Cortex | 0.10814 | 0.00575 | 3 | 11 | 0.14266 |
| Control DG | 0.06283 | 0.00603 | 3 | 11 | |
| Emx1/TeNT DG | 0.07221 | 0.0055 | 3 | 9 | 0.27482 |
| Control CA1 | 0.1196 | 0.02827 | 3 | 10 | |
| Emx1/TeNT CA1 | 0.07585 | 0.00386 | 3 | 10 | 0.70517 |

**Terminal volume (nm^3)**

| | | | | | |
|---|---|---|---|---|---|
| Control Cortex | 8.67E+07 | 8.43E+06 | 3 | 12 | |
| Emx1/TeNT Cortex | 1.67E+08 | 2.49E+07 | 3 | 11 | <0.05 |
| Control DG | 5.62E+07 | 7.36E+06 | 3 | 11 | |
| Emx1/TeNT DG | 1.72E+08 | 2.59E+07 | 3 | 9 | <0.001 |
| Control CA1 | 7.88E+07 | 1.91E+07 | 3 | 10 | |
| Emx1/TeNT CA1 | 1.33E+08 | 1.32E+07 | 3 | 10 | <0.01 |

**Total SVs**

| | | | | | |
|---|---|---|---|---|---|
| Control Cortex | 274 | 52 | 3 | 12 | |
| Emx1/TeNT Cortex | 357 | 61 | 3 | 11 | 0.32 |
| Control DG | 269 | 36 | 3 | 11 | |
| Emx1/TeNT DG | 493 | 67 | 3 | 9 | <0.02 |
| Control CA1 | 229 | 38 | 3 | 10 | |
| Emx1/TeNT CA1 | 317 | 25 | 3 | 10 | 0.074 |

**Tethered SVs**

| | | | | | |
|---|---|---|---|---|---|
| Control Cortex | 11.8 | 1.9 | 3 | 9 | |
| Emx1/TeNT Cortex | 20 | 1.97 | 3 | 9 | <0.01 |
| Control DG | 11.6 | 2.2 | 3 | 9 | |
| Emx1/TeNT DG | 18 | 1.8 | 3 | 9 | <0.05 |
| Control CA1 | 13.6 | 3.25 | 3 | 9 | |
| Emx1/TeNT CA1 | 20.3 | 1.5 | 3 | 9 | 0.0756 |

**Tethered SVs / AZ**

| | | | | | |
|---|---|---|---|---|---|
| Control Cortex | 0.1406 | 0.0151 | 3 | 9 | |
| Emx1/TeNT Cortex | 0.1701 | 0.0166 | 3 | 9 | 0.21 |
| Control DG | 0.149 | 0.0184 | 3 | 9 | |
| Emx1/TeNT DG | 0.1396 | 0.0163 | 3 | 9 | 0.7 |
| Control CA1 | 0.1137 | 0.0234 | 3 | 9 | |
| Emx1/TeNT CA1 | 0.1252 | 0.0085 | 3 | 9 | 0.6522 |